

Interaction Notes

Note 368

October 1976

Angular Variation of Current on  
Moderately Thin Cylindrical Scatterers

B. M. Duff  
University of Mississippi

Abstract

The surface current density induced on finite length cylindrical scatterers, of moderately thin radius, has been investigated experimentally. The results of this investigation clearly show an angular variation of the axially directed current density on cylinders of electrical radius  $ka = 0.04$ . The data has been analyzed to express the current density as a Fourier series in the angle variable  $\phi$ . The results of this analysis show that the angularly independent component is essentially in agreement with solutions based on a thin wire approximation, while the  $\cos(n\phi)$  terms are essentially constant with respect to  $z$ . Comparisons are then made with the known solutions for an infinitely long cylindrical scatterer.

ANGULAR VARIATION OF CURRENT ON  
MODERATELY THIN CYLINDRICAL SCATTERERS

(1) Introduction

Conducting structures composed of electrically thin cylinders (wires) form an important class of problems in electromagnetics. When excited by a source within the structure, these geometries comprise the linear antenna problem. When excited by sources exterior to the structure, they are treated as scatterers. The thin wire scatterer has often been used to obtain a first approximation to more complicated structures, for example, the modeling of an aircraft with the wings, fuselage, tail, and so forth replaced by sections of electrically thin conducting cylinders. In connection with these theoretical solutions, experimental measurements of the current and charge distribution have been made [1,2]. The importance of the electrically thin cylinder arises from simplifications which may be made in analysis of the structure. These simplifications are generally lumped under the term "thin wire approximations". It is always of some importance in both theoretical and experimental investigations to evaluate the effect of the thin wire approximation and the restrictions on electrical radius which are necessary for required accuracy. In the case of driven antenna problems, the thin wire limit is often taken as  $ka \leq 0.01$  where  $k$  is propagation constant,  $a$  is the radius of the cylinder. Experimental measurements on driven antenna

structures with  $ka = 0.04$  have been made and show good agreement with theoretical solutions based on thin wire approximations [1]. An assumption which is common to all thin wire approximations and the one with which the present work is concerned is that the current distribution induced on the structure is independent of the cylindrical angle variable  $\phi$ . As will be shown this assumption is strictly valid, for cylinders of nonzero radius, only when the excitation is itself independent of  $\phi$ . The image plane monopole driven by a TEM mode coaxial line is an example of a  $\phi$  independent excitation. It has been recognized, however, that in a scattering problem for which the excitation is an incident electromagnetic wave the assumption of angular independence of the current is not strictly valid. (For a discussion of this effect related to the EMP problem, see reference 3.)

The necessity for a  $\phi$  dependence of the current distribution induced on a conducting cylinder by an incident plane wave may be seen from an examination of the boundary conditions on the  $\bar{H}$  field. Referring to Fig. 1, the important boundary condition is

$$\hat{n} \times \bar{H} = \bar{J}_s \quad (1.1)$$

where

$\hat{n}$  = the unit normal to the surface

$\bar{H}$  = the total  $\bar{H}$  field

$\bar{J}_s$  = the induced surface current

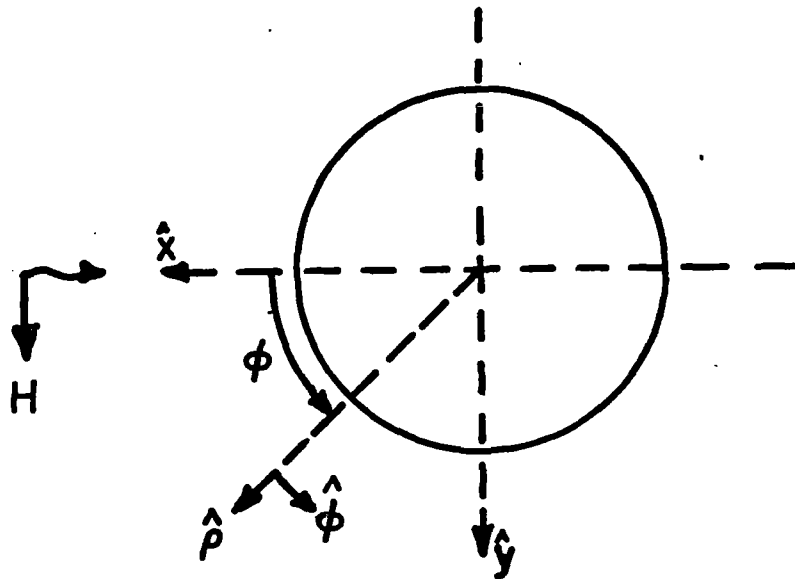


Figure 1 Geometry for Cylinder Illuminated by a Plane Wave

Expressing the total  $\bar{H}$  field as a combination of incident and scattered fields, we obtain

$$\hat{n} \times \bar{H} = \hat{n} \times \bar{H}^i + \hat{n} \times \bar{H}^s \quad (1.2)$$

For a TM plane wave illumination the incident field may be expressed as

$$\begin{aligned} \bar{H}^i &= H_0 e^{-jkx} \hat{y} \\ \bar{H}^i &= H_0 \cos\phi e^{-jk\rho \cos\phi} \hat{\phi} \end{aligned} \quad (1.3)$$

and

$$\hat{n} \times \bar{H}_s = \bar{J}_s - H_0 \cos\phi e^{-jka \cos\phi} \hat{\phi} \quad (1.4)$$

From Eq. (1.4) it is seen that if we assume  $\bar{J}_s$  to be independent of  $\phi$  then  $\bar{H}^s$  at the surface must have a  $\phi$  dependence. However,  $\bar{H}^s$  may be computed as the field having  $\bar{J}_s$  as its source. By symmetry a  $\phi$  independent  $\bar{J}$  can produce only a  $\phi$  independent  $\bar{H}^s$ , and thus a contradiction is reached. It must, therefore, be concluded that the surface current induced on a nonzero radius cylinder by an incident plane wave must have a  $\phi$  variation. In addition to the above analysis, it is instructive to examine the solution for an infinitely long cylindrical scatterer. It is well known that the current distribution on the infinite long cylinder may be expressed as a Fourier series in the angle variable  $\phi$  [4].

The necessity for the induced current to have a  $\phi$  variation is often overlooked in both theoretical and experimental work. The extent to which the angular variation affects the results of course depends on the

specific problem being studied. The investigation reported in the following sections was initiated at this laboratory as a result of observations made during a study of a V-cross scattering structure having  $ka = 0.04$ . It was observed that a  $180^\circ$  rotation of the structure and hence of the measuring probe resulted in significant differences in the measured currents. The measured current distribution of the V-cross scatterer are shown in Figs. 2a and 2b. From this data it can be seen that the variation in current between  $\phi = 0^\circ$  and  $\phi = 180^\circ$  is quite significant on some portions of the structure. In order to obtain a better understanding of these effects a series of measurements on straight cylindrical scatterers of  $ka = 0.04$  has been conducted with emphasis on determining the nature of the  $\phi$  variation. The results of this investigation are reported in the following sections.

(ii) Measurement Techniques

The cylindrical scatterer system used for this investigation is shown in Fig. 3. The scatterer is constructed from brass tubing of radius 3.175 mm mounted perpendicular to a large vertical image plane (5.5 m by 8.5 m). The tube is slotted axially to provide for movement of the measuring probe except for the last 1 cm at the end of the tube. The end of the tube is unslotted to provide a continuous conducting surface for a  $\phi$  directed current which may exist near the end of the tube. This test structure is illuminated by a transmitting antenna composed of a dipole mounted in a  $90^\circ$  corner reflector located at a distance of about 10 wave-

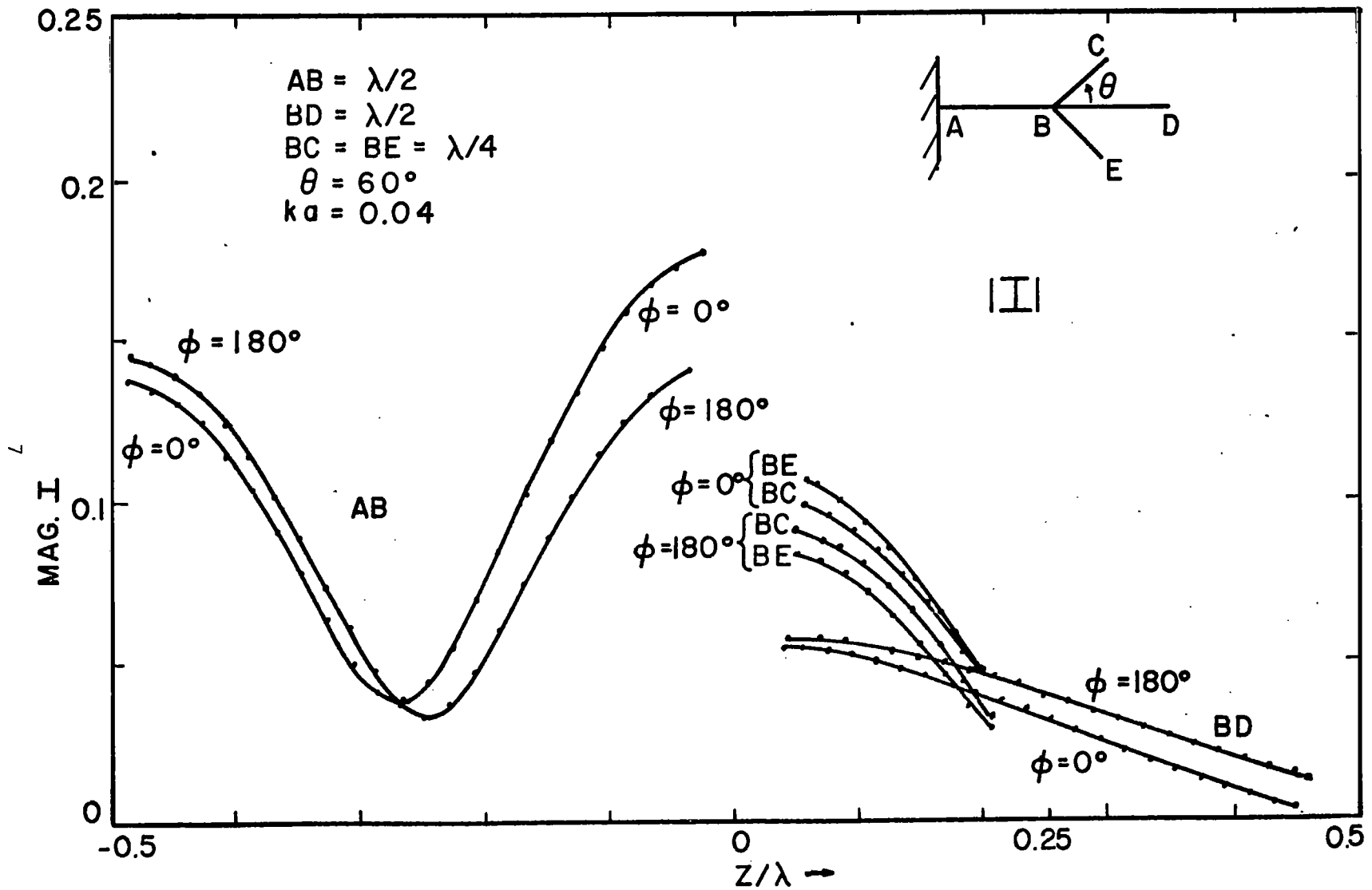


Figure 2a Magnitude of Current on V-Cross Scatterer,  $\phi = 0^\circ$  and  $\phi = 180^\circ$

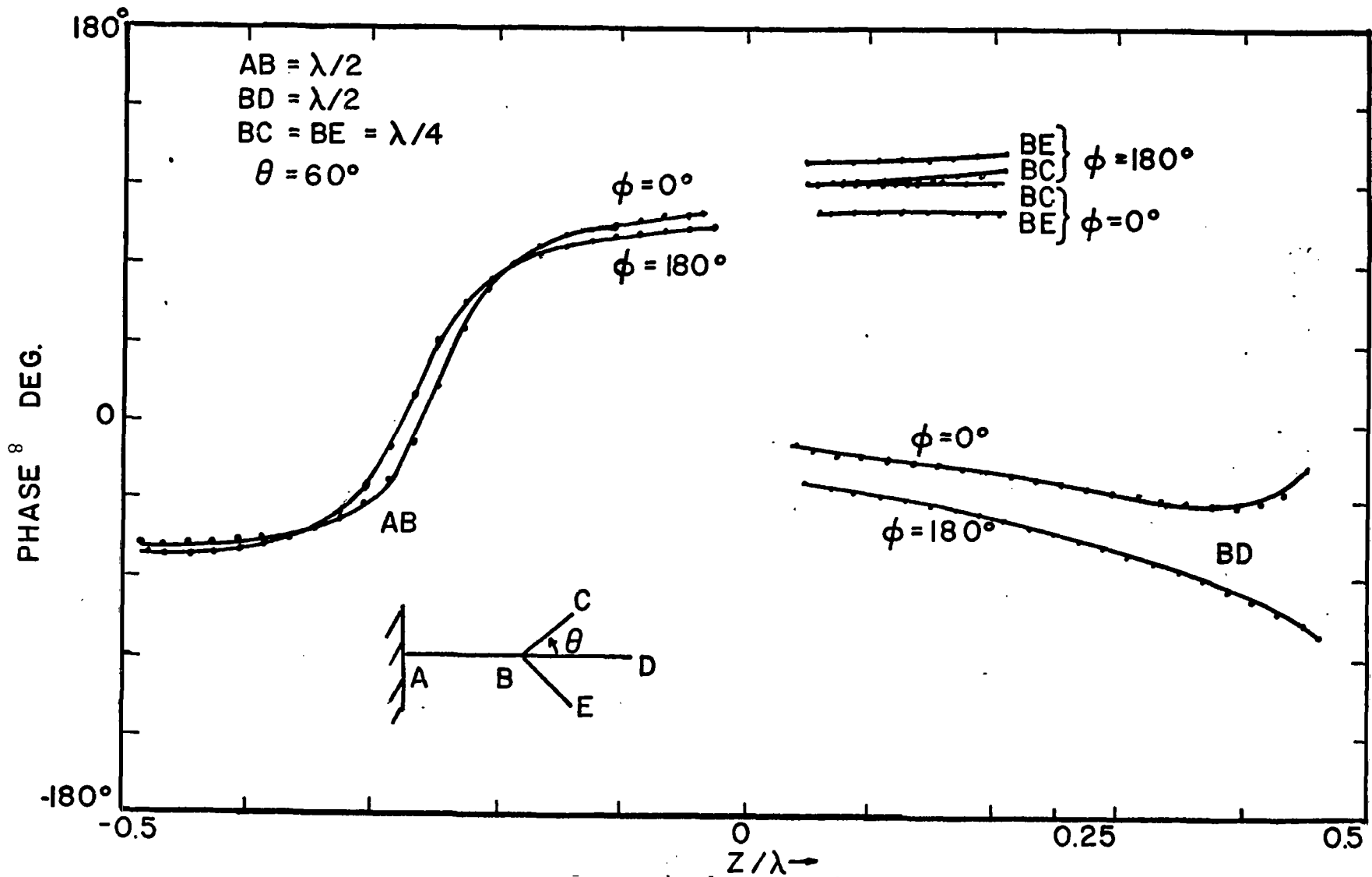


Figure 2b Phase of current on V-Cross Scatterer,  $\phi = 0^\circ$  and  $\phi = 180^\circ$



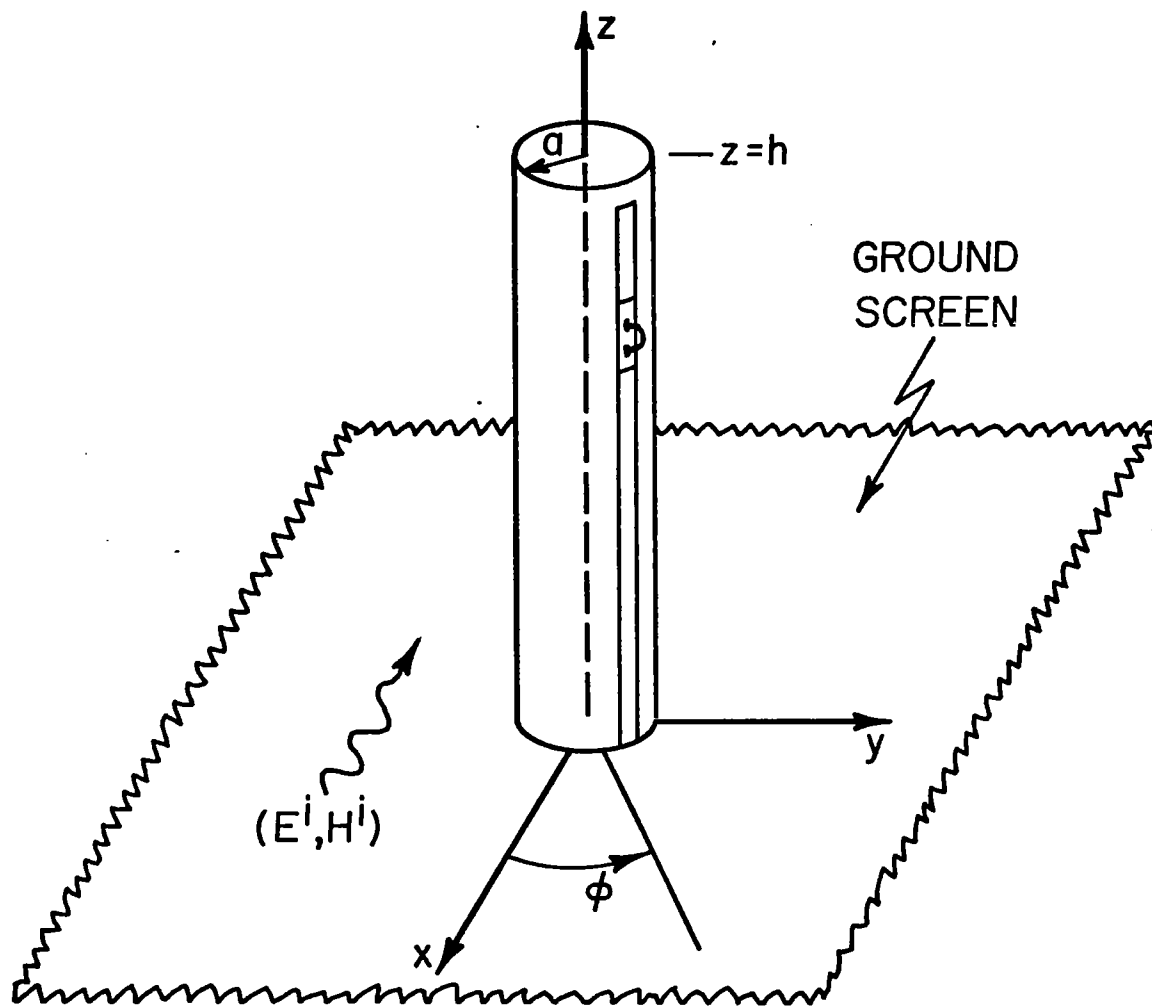


Figure 3 Diagram of Cylindrical Scatterer over Image Plane

lengths from the test structure. A frequency of 600 MHz was chosen for the incident field giving a free space wavelength of  $\lambda = 50$  cm. At this frequency the image plane is  $11\lambda$  by  $17\lambda$  and the electrical radius of the scatterer is  $ka = 0.04$ . The test structure was mounted on a rotatable disk in the image plane. Rotation of the entire structure thus effectively places the probe at different  $\phi$  positions around the cylinder.

The current distribution was measured using a center loaded loop probe 3.175 mm diameter and constructed from Cable-Wave UT-20 coaxial cable. The probe is oriented to measure  $H_\phi$  and hence the axial component of current. The signal cable from the probe passes through a 1.59 mm radius tube which is fastened to the probe carriage and runs inside of the test cylinder to instrumentation behind the image plane. This small tube is coated with an absorbing material to reduce the possibility of fields being excited on the interior of the test cylinder.

During the measurements, the incident field is monitored by a short monopole located on the image plane approximately 1 m from the test structure and at the same distance from the transmitter as the test structure. The signal received from this probe is used to correct the measurements on both amplitude and phase for drifts in the incident field illumination.

Signal from the current probe is measured using a HP 8405A vector volt meter. The magnitude and phase outputs of the vector volt meter are measured with a HP 3490 digital volt meter which is interfaced to a HP 9820 calculator. All measurements are conducted under program control by the calculator and the data, after corrections for drifts of incident field, are stored in the calculator for later analysis and plotting.

As in any measurement it is important to understand the response of the measurement probe and its relation to the quantity being measured. A sufficiently small center loaded loop antenna responds essentially to the total magnetic flux over the area of the loop [5]. From the boundary condition Eq. (1.1), it is seen that the total tangential magnetic field at the surface of the conductor is equal to the surface current density. Since the signal induced in the probe is taken as being proportional to the surface current density, errors may be introduced because of the finite size of the probe. The incident field component is a very slowly varying function over the dimensions of the probe. It is, therefore, only the scattered components of the total field which may produce significant errors. Rapid spatial variations of the scattered field, however, can only occur near discontinuities or changes in geometry of the conducting surfaces which in the present problem only occur near the end of the tube. Since measurements were made only to within 4.25 tube radii and 8.5 probe radii of the end, the errors over the measurement region are small.

On all sliding surfaces, i.e., probe carriage and rotating disk, a conducting grease compound was used to insure good electrical contact. Tests were conducted with these areas covered by conducting tape. No significant change in the measured signal was observed. The conducting grease was, therefore, assumed to provide adequate electrical continuity.

Measurements of the surface current density were made at 1 cm intervals in  $z$  and  $45^\circ$  intervals in  $\phi$  over the surface of the cylinder. The resulting data are presented in the following section.

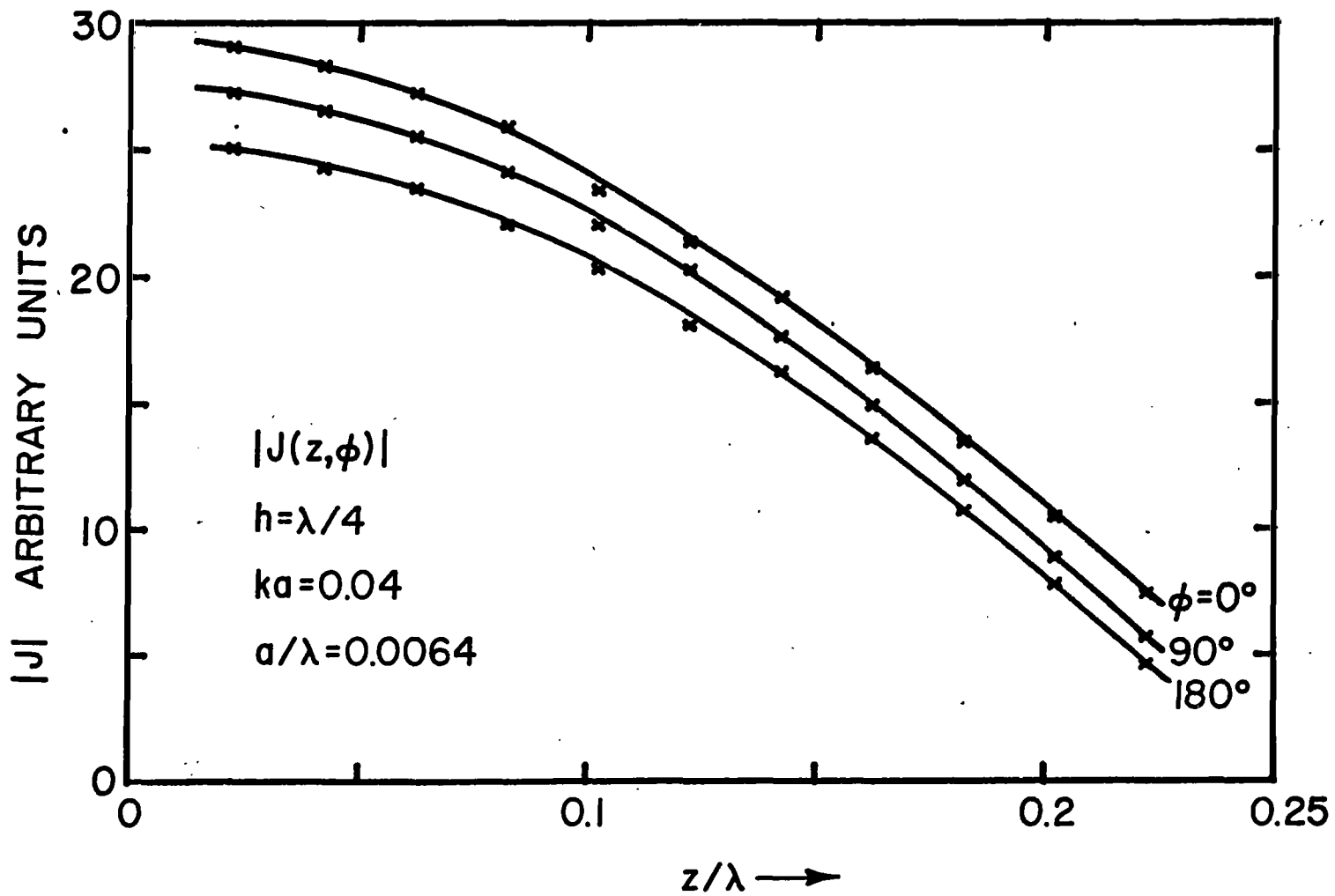
(iii) Measured Data and Analysis

The magnitude and phase of the measured current density distributions for finite length conducting cylinders of  $ka = 0.04$  are shown in Figs. 4 - 7 as a function of  $z$ , with  $\phi$  as a parameter. Four different lengths of cylinder were studied having  $h = \lambda/4, \lambda/2, 3\lambda/4,$  and  $\lambda$ . Although data were recorded at  $5^\circ$  intervals in  $\phi$  for the full  $360^\circ$  range, only data for  $\phi = 0^\circ, 90^\circ,$  and  $180^\circ$  are presented since no unusual behavior was observed at the other angles. Although it can be seen that the angular variation of the current is pronounced for all lengths studied, the effects may be seen to differ in some respects as a function of  $h$ . Further discussion of this  $h$  dependence is contained in the next section.

From the solution for scattering by an infinite length cylinder [4] and studies of an electrically thick cylinder [6], it appears that a Fourier series expansion in the variable  $\phi$  is an appropriate means of analyzing the data. The surface current density may, therefore, be expressed as

$$J_z(z, \phi) = J_0(z) + J_1(z) \cos \phi + J_2(z) \cos n\phi + \dots \quad (1.5)$$

where only  $\cos(n\phi)$  terms are included since these are the only terms to be expected if the geometry of Fig. 3 is maintained in the experimental system. With the aid of a computer the coefficients of Eq. (1.5) were computed from the measured data. The actual analysis included computation of  $\sin(n\phi)$  coefficients as a test of the accuracy of the experimental system. In all cases, the computed  $\sin(n\phi)$  coefficients were very small and are believed

Figure 4a Magnitude of Current Density,  $h = \lambda/4$

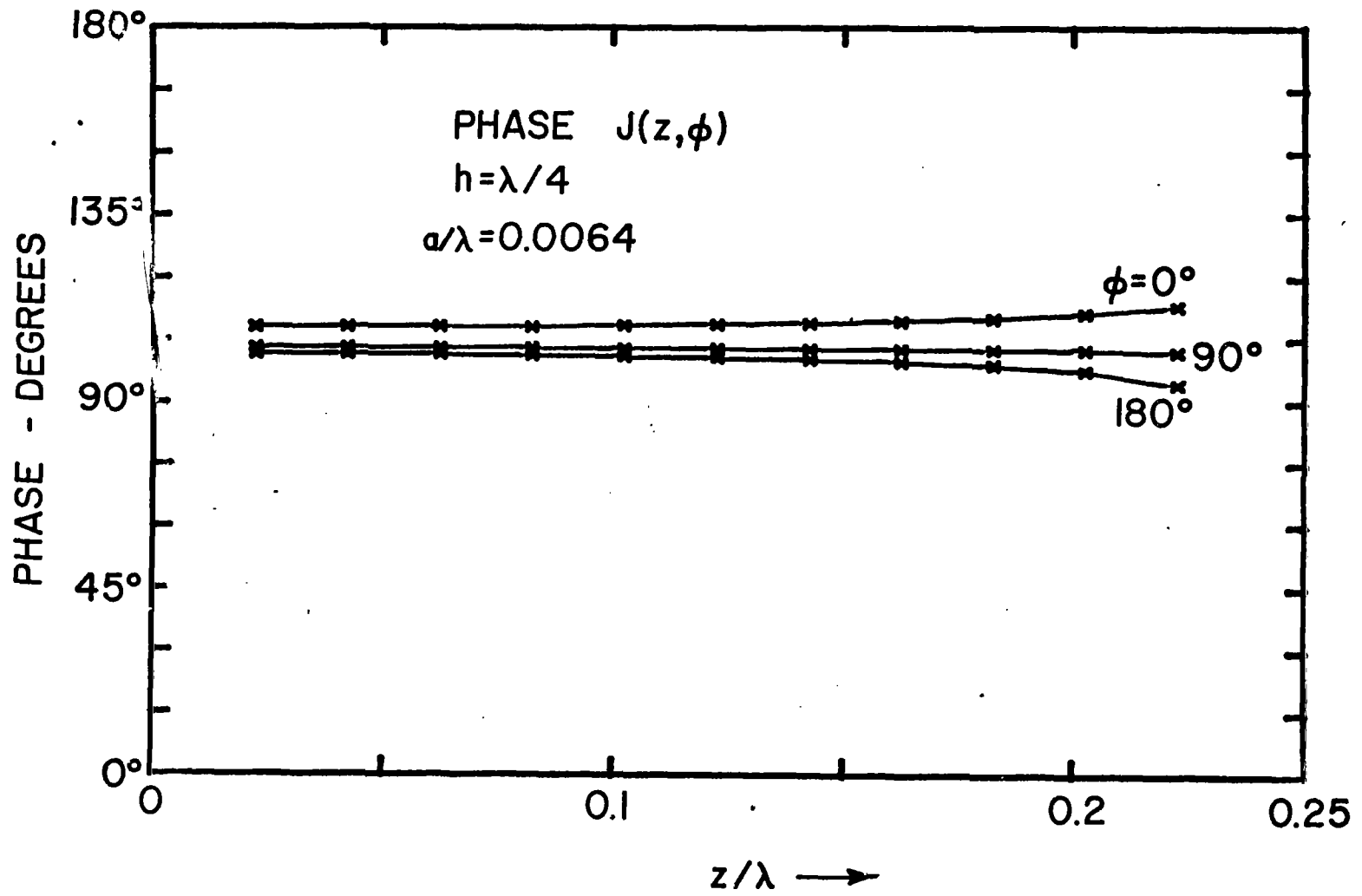


Figure 4b Phase of Current Density,  $h = \lambda/4$

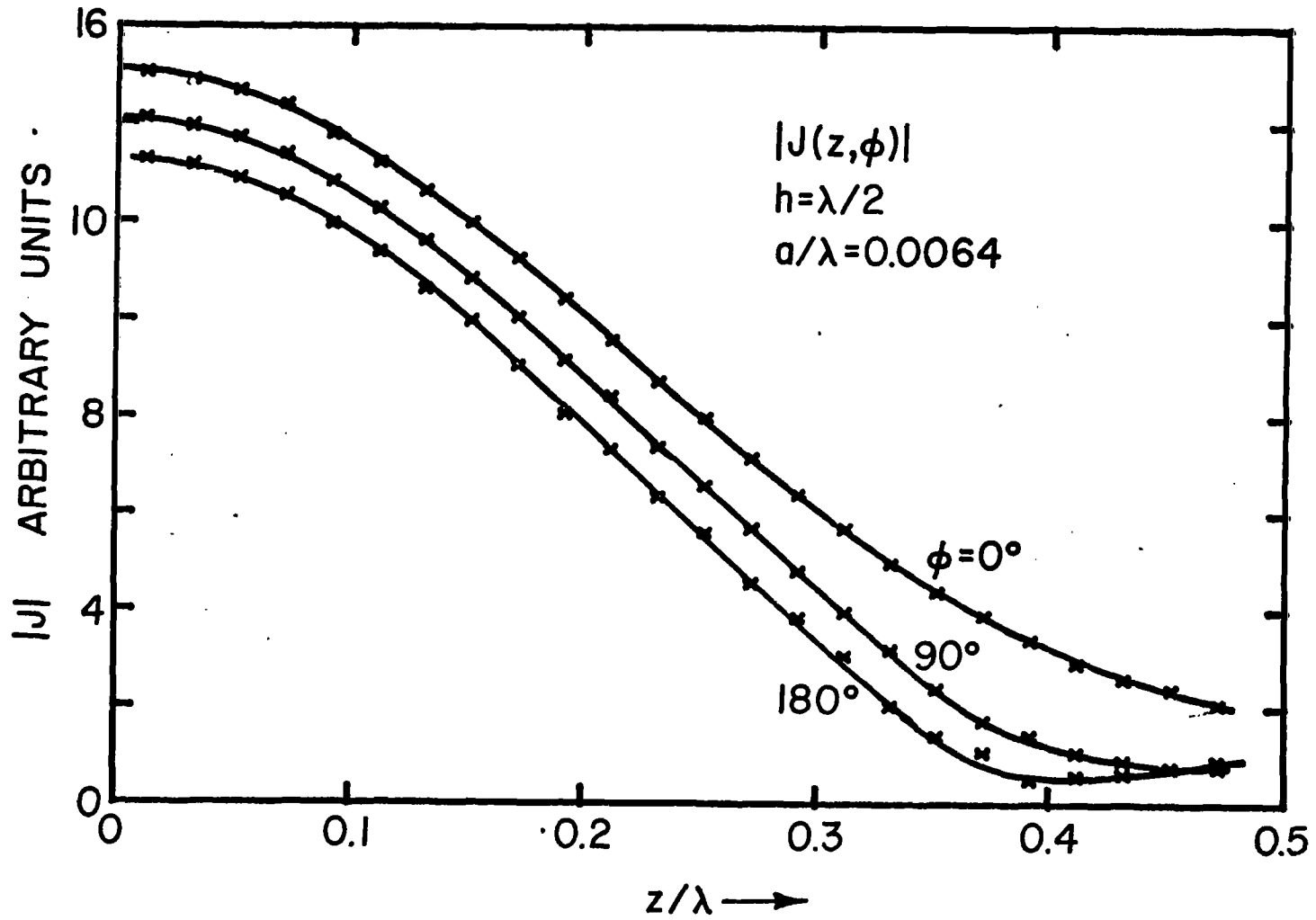
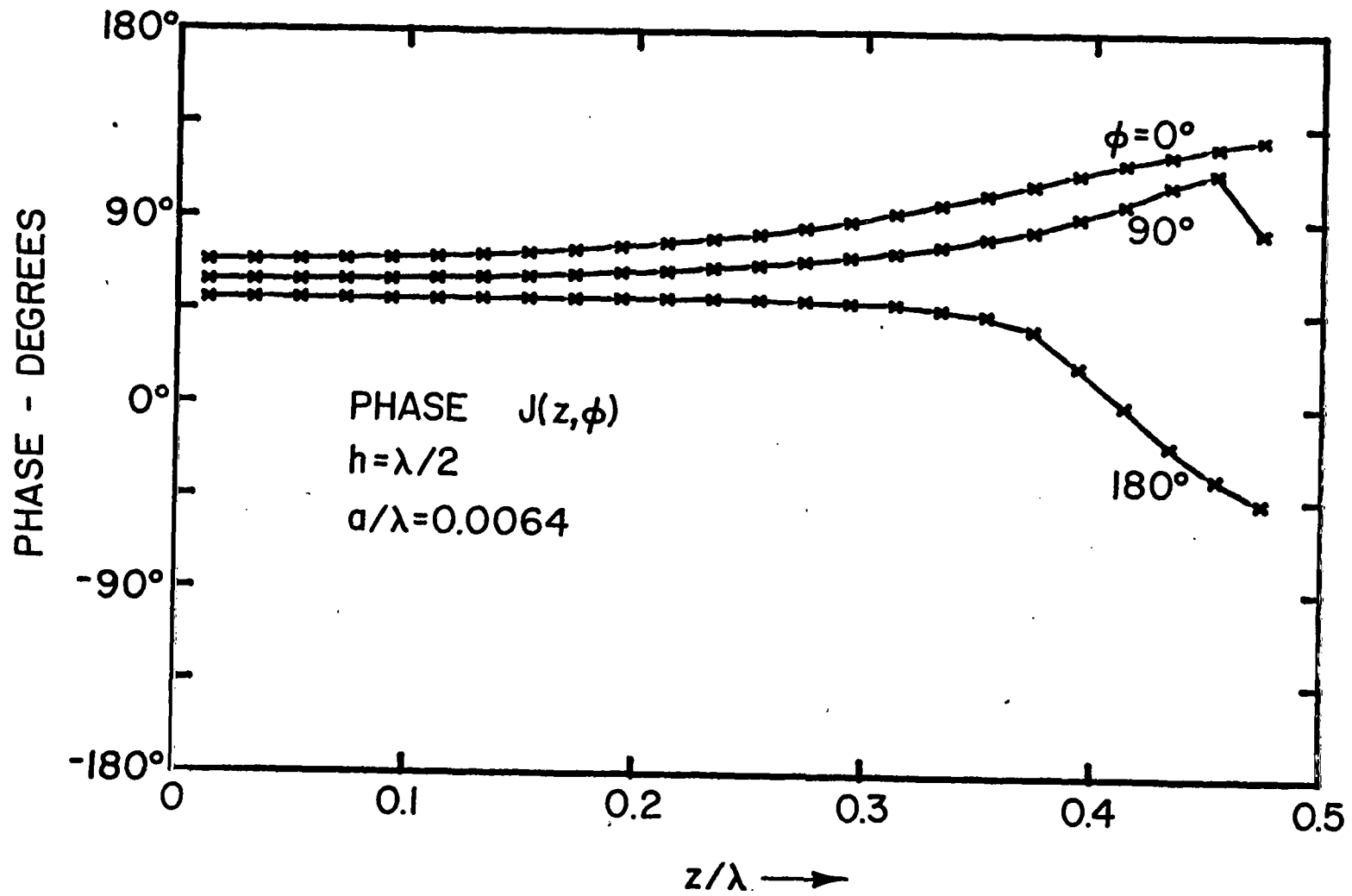


Figure 5a Magnitude of Current Density,  $h = \lambda/2$

Figure 5b Phase of Current Density,  $h = \lambda/2$



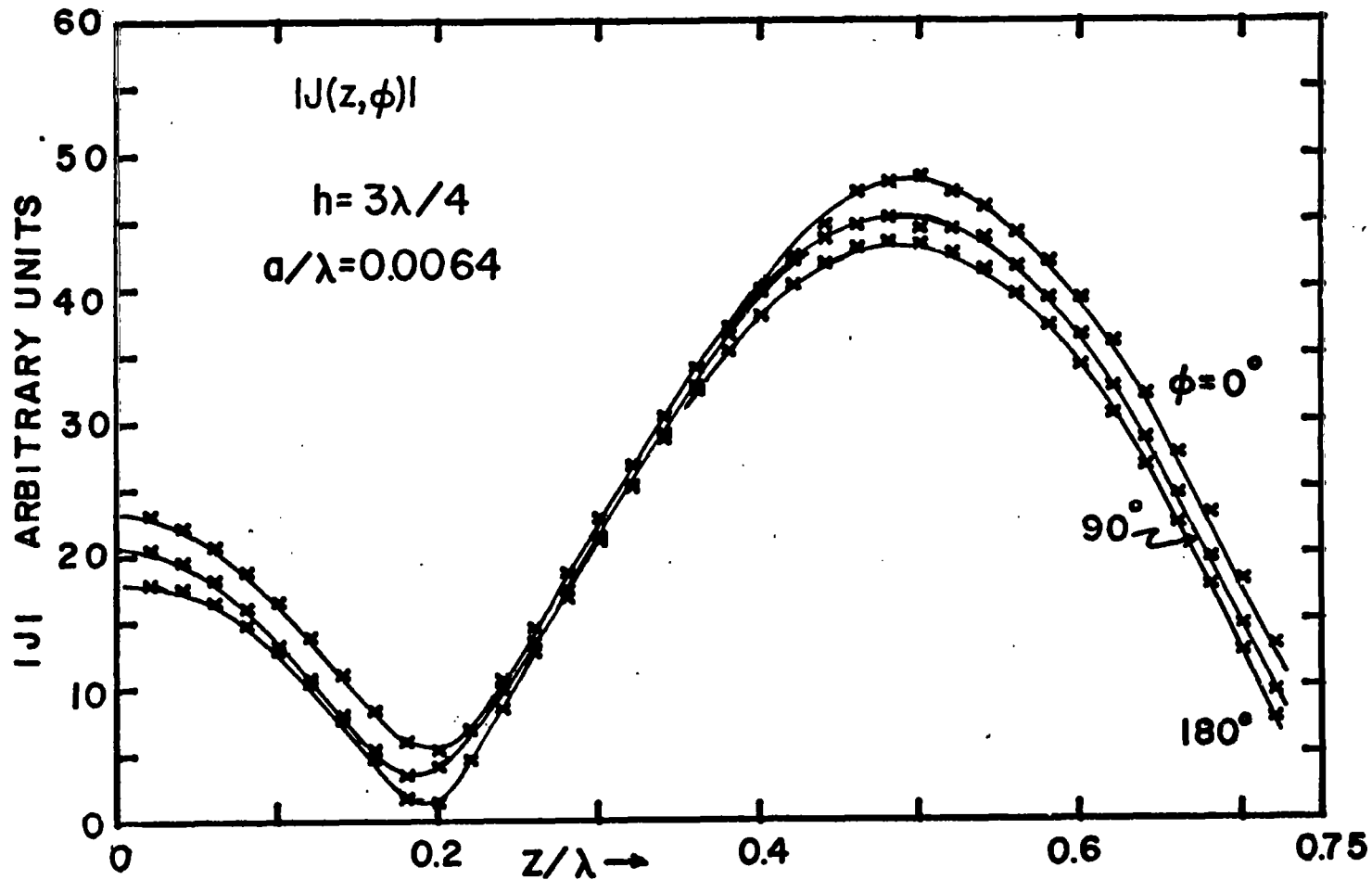


Figure 6a Magnitude of Current Density,  $h = 3\lambda/4$

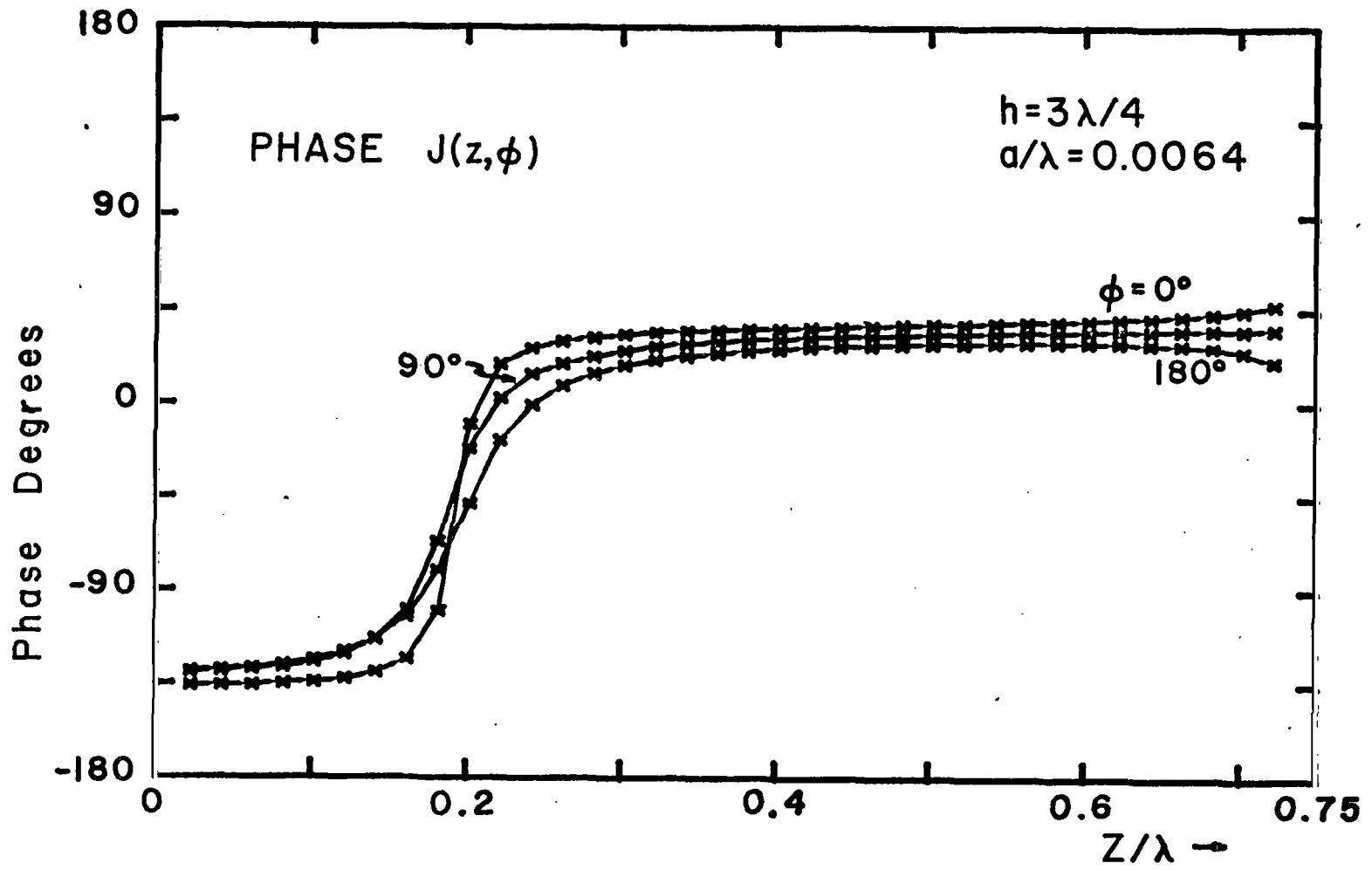


Figure 6b, Phase of Current Density,  $h = 3\lambda/4$

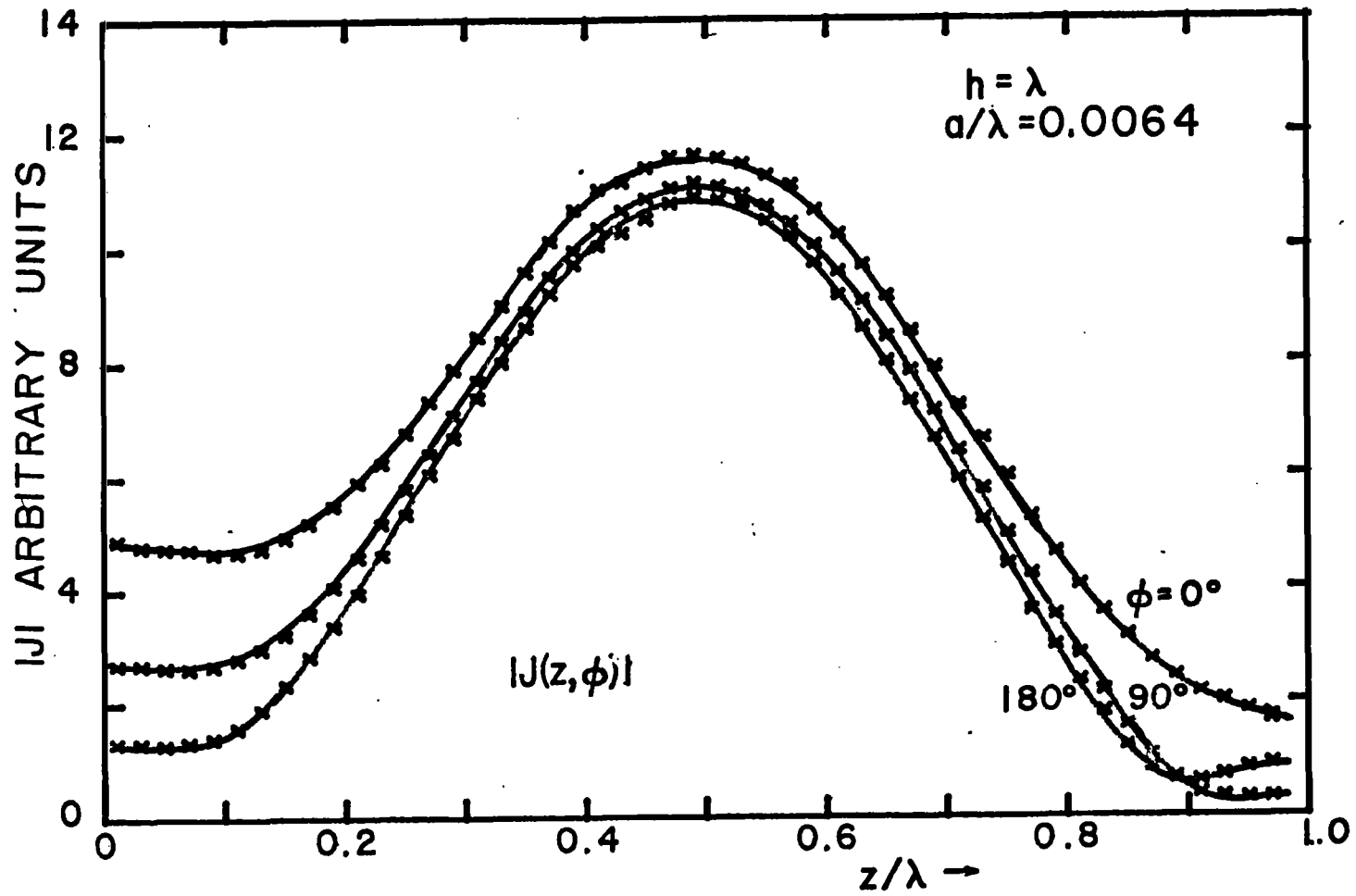


Figure 7a Magnitude of Current Density,  $h = \lambda$

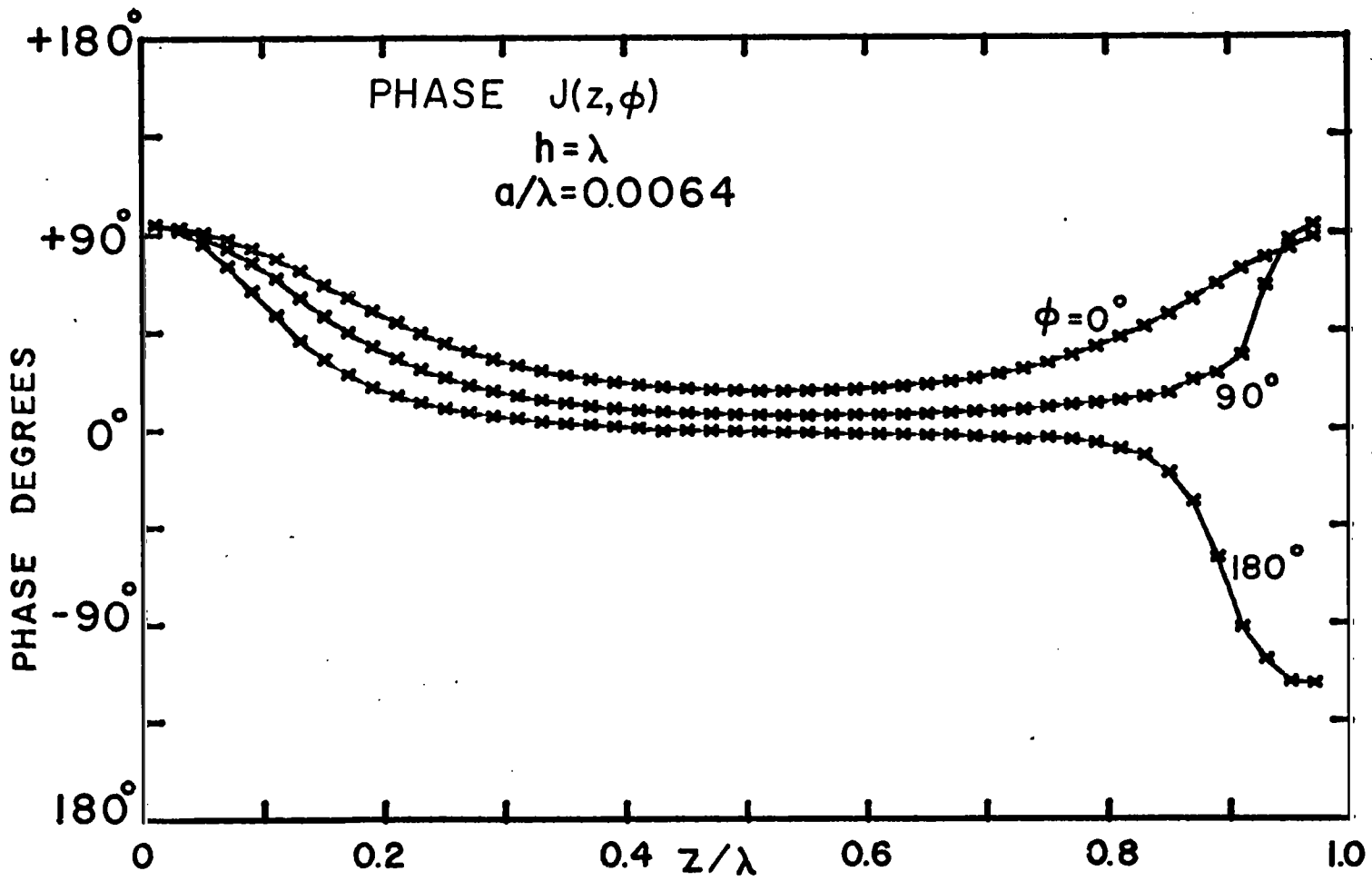


Figure 7b Phase of Current Density,  $h = \lambda$

to result as much from noise as from any real features of the measured current density. The computed  $J_n(z)$  coefficients are shown in Figs. 8, 9, 10, and 11.

(iv) Conclusions

At the present time no theoretical solution for scattering from finite length cylinders of moderately thin size is available for comparison with the measured data presented here. Some conclusions and understanding of the behavior of the current distribution can be drawn, however, from the measured data and may serve as a guide to the formulation of an approximate theoretical treatment.

The general behavior of the current density is found to be greatly dependent on the length  $h$  of the cylinder as was pointed out above. This height effect is seen from a comparison of Figs. 4 and 6 with Figs. 5 and 7. Figs. 4 and 6 for  $h = \lambda/4$  and  $3\lambda/4$ , respectively, show a  $\phi$  variation in both magnitude and phase of the current density but show very similar  $z$  dependence for all values of  $\phi$ . In contrast, Figs. 5 and 7 for  $h = \lambda/2$  and  $\lambda$ , respectively, show a significant change in  $z$  dependence for different  $\phi$  positions especially near the end of the cylinder. The most striking feature of these current distributions is that the axially directed current does not approach zero toward the end of the cylinder. In fact, the data for both  $h = \lambda/2$  and  $\lambda$  shows that the magnitude of  $J_z$  at  $\phi = 180^\circ$  reaches a minimum and then increases toward the end. The explanation for the end behavior of  $J_z$  and the differences in behavior as a function of  $h$  is most easily understood from an examination of the Fourier components

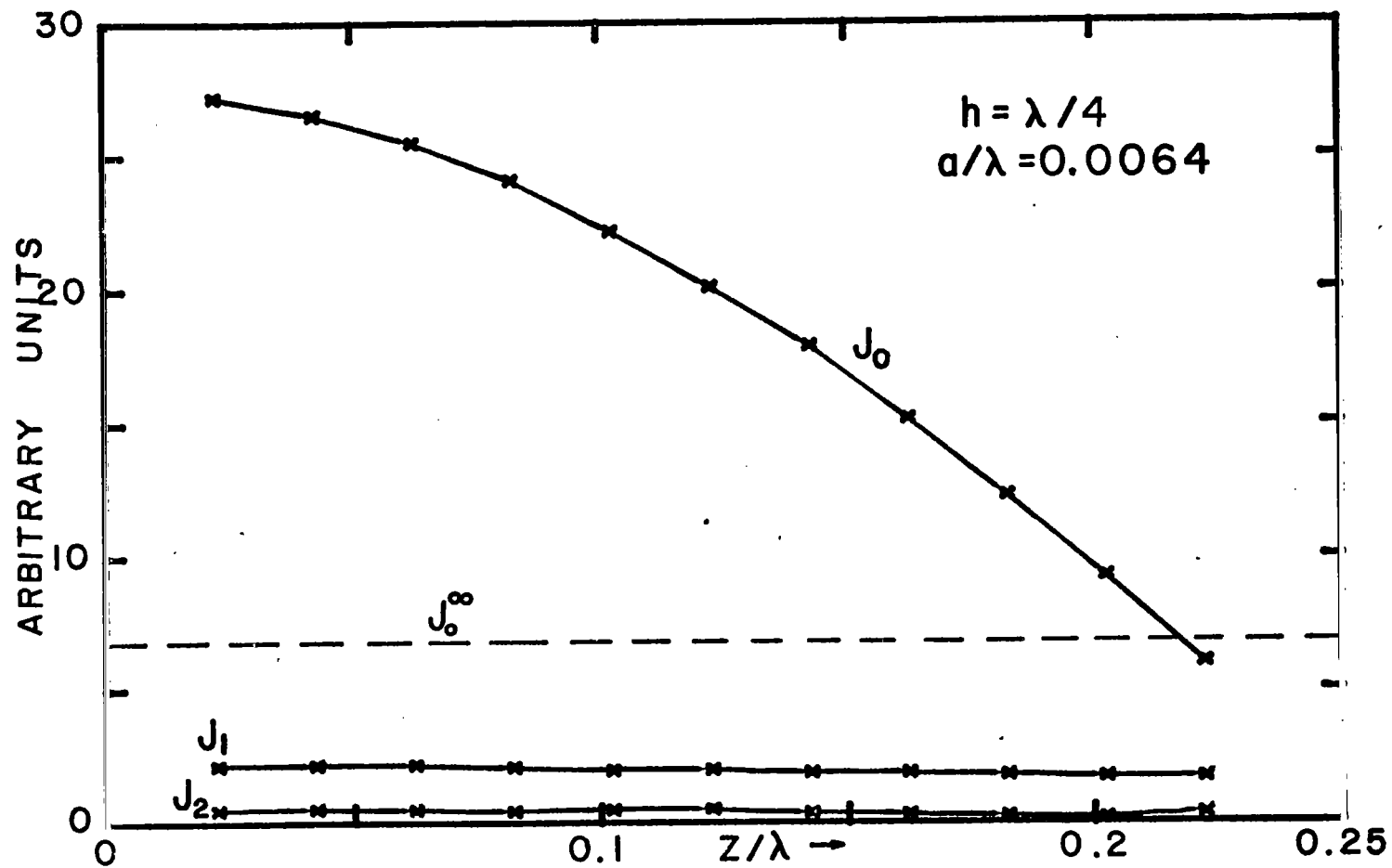


Figure 8 Fourier Components of Current Density,  $h = \lambda/4$

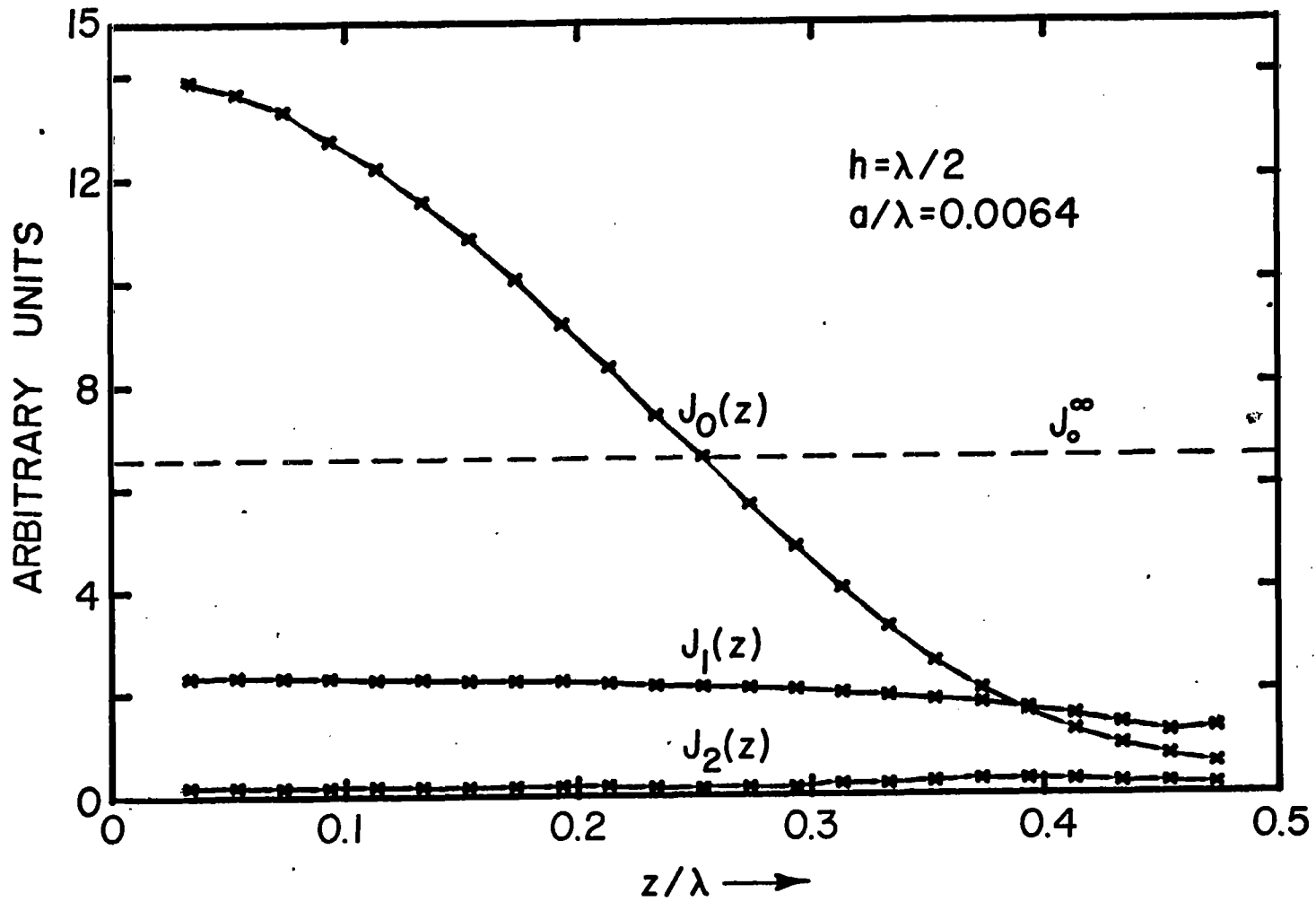


Figure 9 Fourier Components of Current Density,  $h = \lambda/2$

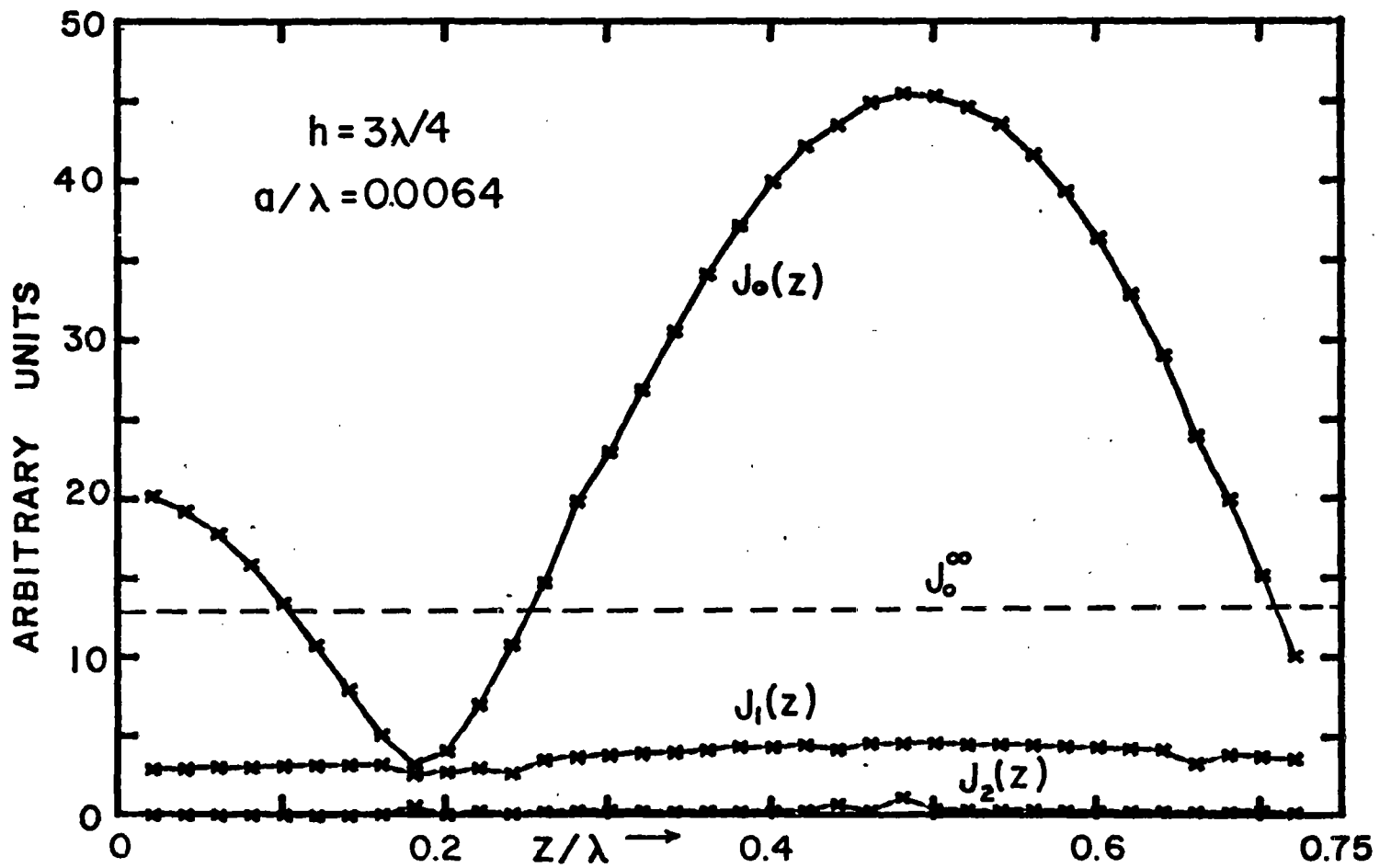


Figure 10 Fourier Components of Current Density,  $h = 3\lambda/4$



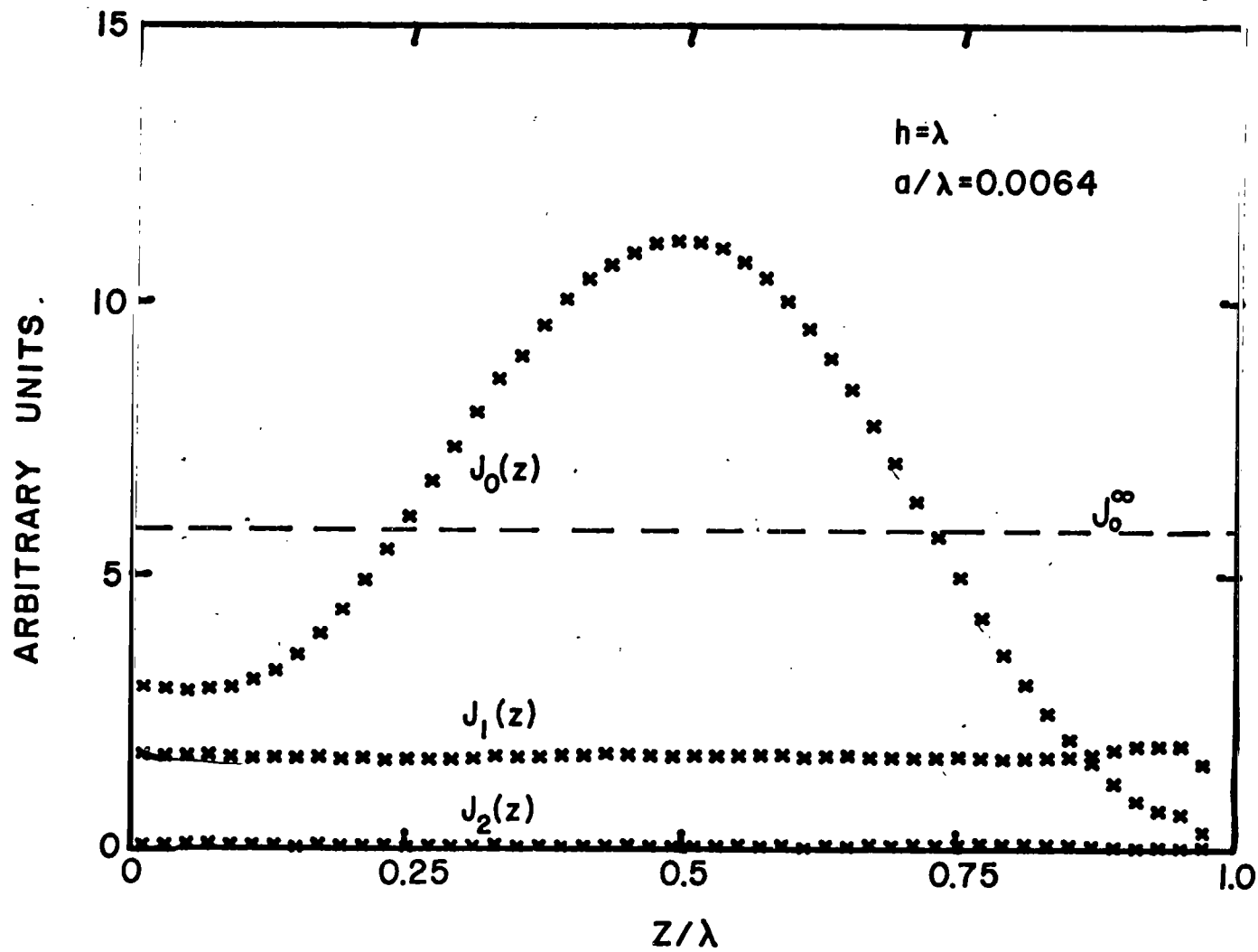


Figure 11 Fourier Components of Current Density,  $h = \lambda$

shown in Figs. 8 - 11. For all cases studied the  $J_1(z)$ , i.e.,  $\cos\phi$ , coefficient is essentially constant as is  $J_2(z)$ . The cylinders of length  $h = \lambda/4$  and  $3\lambda/4$  are of resonant length and the  $J_0(z)$ , i.e., angularly independent, component is seen to be the typical resonant current distribution which is approximated by  $\sin k(h-z)$ , thus for the resonant length the  $J_0(z)$  component is not only large in magnitude but approaches zero toward the end with a large slope. Over the range of  $z$  for which data are available  $J_0$  remains large compared to  $J_1$ . The lengths  $h = \lambda/2$  and  $\lambda$ , on the other hand, are antiresonant and  $J_0(z)$  is seen to be essentially the forced response of the general form  $(1 - \cos k(h-z))$ . This forced current distribution is not only smaller in magnitude relative to  $J_1$  than the resonant currents but approaches zero toward  $z = h$  with zero slope. Thus, for the antiresonant cases  $J_1$  becomes the largest component over a distance of about  $0.1\lambda$  near the end. This predominance of the  $J_1$  component near the end explains the behavior of the total current density observed in Figs. 5 and 7. Since it is believed that the  $J_1$  and all higher order coefficients will remain essentially constant to  $z = h$ , a sudden change in the phase of the current would also be expected very near the end for the resonant cases,  $h = \lambda/4$  and  $3\lambda/4$ , if it were possible to obtain measurements in this region.

The constancy with respect to  $z$  of  $J_1(z)$  and higher order coefficients is to be expected since these components may be considered as directly excited by the incident field and must exist in order to satisfy the boundary conditions. The behavior of these components at the end of the

cylinder, however, deserves some consideration. From the analysis of electrically thick cylinder [6], it is found that a  $\phi$  directed component of current exists near  $z = h$ . It is reasonable to assume, therefore, that some  $\phi$  directed component of current will exist near the end of any non-zero radius cylindrical scatterer. Furthermore, in accordance with the edge condition, this  $\phi$  directed component must be singular at  $z = h$ . Thus, it appears that the angularly dependent Fourier components of the  $z$  directed current are essentially constant for all  $z$ ; the total current, however, becoming  $\phi$  directed at  $z = h$ .

Further information concerning the observed distribution may be obtained from a comparison with the known solution for infinitely long cylinders. The induced current density on an infinite cylinder illuminated by a plane wave may be expressed as [4]

$$J_z(\phi) = \frac{2E_0}{\omega\mu\pi a} \sum_{n=-\infty}^{\infty} \frac{j^{-n} e^{jn\phi}}{H_n^{(2)}(ka)} \quad (1.6)$$

where  $H_n^{(2)}(ka)$  is the Hankel function of the second kind. Combining terms, Eq. (1.6) becomes;

$$J_z(\phi) = \frac{2E_0}{\omega\mu\pi a} \left[ \frac{1}{H_0^{(2)}(ka)} - j \frac{2}{H_1^{(2)}(ka)} \cos\phi - \frac{2}{H_2^{(2)}(ka)} \cos\phi + \dots \right] \quad (1.7)$$

which is of the same form as the Fourier series expansion of Eq. (1.5).

Using small argument approximations for the Hankel functions, the relative magnitude of the Fourier coefficients for  $ka = 0.04$  are found to be

$$J_0^\infty \doteq 3.38 J_1^\infty$$

$$J_2^\infty \doteq 0.02 J_1^\infty \tag{1.8}$$

Since no absolute value of the incident field illumination was available for the measured data, it is not possible to compare the actual magnitudes of current with the equivalent results for infinite cylinder. However, taking the values measured for  $J_1$  it is possible to compute an equivalent value of  $J_0^\infty$ . The computed values of  $J_0^\infty$ , obtained from the average measured values of  $J_1$ , are shown as horizontal dashed lines in Fig. 8 - 11. It is seen that for the antiresonant lengths  $h = \lambda/2$  and  $\lambda$  the equivalent  $J_0^\infty$  is very nearly the mean value of the measured  $J_0(z)$  component. As expected, however, the equivalent value of  $J_0^\infty$  is much less than the mean value of the measured  $J_0(z)$  for the resonant lengths  $h = \lambda/4$  and  $3\lambda/4$ .

The results of this investigation clearly establish the existence of an angular variation of the induced current on electrically thin cylindrical scatterers. It is evident, therefore, that, for at least some applications, solutions based on the conventional thin wire approximation will be inadequate. Furthermore, it is apparent that care must be taken in performing measurements on thin cylindrical scatterers. Measurements of the current distribution which are made at a single arbitrarily chosen angular position may be misleading, particularly when compared with thin wire solutions. The measured data, however, indicate that the  $J_2$  and higher order components are very small. Measurements conducted at  $\phi = 90^\circ$  will, therefore, provide

sufficient information about the angularly independent component,  $J_0$ , and hence the total current. For more complete information, the current density should be measured at  $\phi = 0^\circ$  and  $\phi = 180^\circ$ .

In conclusion, the observations drawn from the measured data suggest that an approximate solution for thin cylindrical scatterers might be obtained by a combination of a thin wire approximation and the solution for an infinite length cylinder.

### References

1. R. B. Mack, A Study of Circular Arrays, Cruft Laboratory Report 384, Harvard University, Cambridge, Massachusetts; 1963.
2. R. W. Burton and R. W. P. King, "Measured Currents and Charges on Thin Crossed Antennas in a Plane-Wave Field," Trans. IEEE, Vol. AP-23, pp. 657-664; September, 1975, and also Interaction Note 258, September 1975.
3. M. I. Sancer, R. W. Latham, and A. D. Varvatis, "Relationship Between Total Currents and Surface Current Densities Induced on Aircraft and Cylinders," AFWL EMP Interaction Note 194; August, 1974.
4. R. F. Harrington, Time Harmonic Electromagnetic Fields, McGraw-Hill Book Company, p. 232; 1961.
5. H. Whiteside, Electromagnetic Field Probes, Cruft Laboratory Technical Report No. 377, Harvard University, Cambridge, Massachusetts; 1962.
6. C. C. Kao, "Three-Dimensional Electromagnetic Scattering from a Circular Tube of Finite Length," Journal of Applied Physics, Vol. 40, pp. 4732 - 4740; November, 1969.